Journal of Nuclear Materials 390–391 (2009) 412–416

Contents lists available at ScienceDirect

Journal of Nuclear Materials

journal homepage: www.elsevier.com/locate/jnucmat

SOLPS5 simulations of Type I ELMing H-mode at JET

B. Gulejová [b,*], R.A. Pitts [b], D. Coster [c], X. Bonnin [d], M. Beurskens [e], S. Jachmich [f], A. Kallenbach [c], contributors to the EFDA-JET workprogramme [a,1]

[a] JET-EFDA, Culham Science Centre, OX14 3DB, Abingdon, UK
[b] CRPP-EPFL, Association EURATOM-Confederation Suisse, CH-1015 Lausanne, Switzerland
[c] Max-Planck Institut für Plasmaphysik, Boltzann str. 2, D-85478, Garching, Germany
[d] LIMHP, CNRS-UPR, Université Paris 13, 99 av. JB Clément, 93430 Villetaneuse, France
[e] Euratom/UKAEA Fusion Association, Culham Science Centre, Abingdon 0X14 3DB, UK
[f] LPP, ERM/KMS, Association Euratom-Belgian State, B-1000, Brussels, Belgium

ARTICLE INFO

PACS:
52.40.Hf
52.55.−s
52.55.Dy
52.55.Fa

ABSTRACT

This paper aims to contribute both to the ongoing process of scrape-off layer code-experiment and code–code benchmarking. Results are presented from SOLPS5 simulations of two high power JET H-modes with similar magnetic configuration, concentrating in the first case on the ELM-free phase of high Ip, ~8 MJ stored energy plasmas with ELMs approaching 1 MJ, modeled for the first time with this code package. A second pulse, with lower stored energy and smaller ELMs, originally considered in detail by Kallenbach with the EDGE2D-NIMBUS code package [Kallenbach et al., Plasma Phys. Control. Fus. 46 (2004) 431], has been modeled as a benchmarking exercise featuring a high level of complexity including carbon impurities and the full ELM cycle. Good agreement is found between the code results. The SOLPS5 results are used to analyse the energy balance during the ELM cycle. In both H-mode discharges, a strong inward particle pinch in the pedestal region is found to be necessary to match measured upstream profiles.

1. Introduction

The SOLPS5 plasma fluid (B2.5)-neutral Monte-Carlo (EIRENE) code package [2] has long been used for simulations of the ITER divertor and scrape-off layer plasma [3]. Yet attempts to carefully match code output against experimental data for specific tokamak discharges on today's machines are still relatively scarce. This paper contributes to the ongoing process of code-experiment and code-code benchmarking by presenting results from SOLPS5 modeling of two separate H-mode pulses, in one case simulating the ELM-free phase of a high power/stored energy discharge with large ELMs and, in the second, modeling the full ELM cycle of lower power H-mode discharge previously examined in detail with the EDGE2D-NIMBUS code package [1]. The good level of agreement between results from the two codes is encouraging given the relatively high level of complexity of the benchmark. It is also one of the rare occasions on which a time-dependent ELM simulation has been performed with SOLPS5 (others may be found in [4,5]). The time independent simulations of the higher power discharge, characterised by extremely large ELMs, form a good basis on which to progress future ELM simulations.

2. Experiment

The two JET discharges considered here are very similar in terms of magnetic configuration, both close to the Diagnostic Optimised Configuration (DOC) plasmas developed for the study of pedestal and SOL physics during ELMing H-mode [6]. They are both vertical target equilibria with moderate triangularity ($\delta \sim 0.25$) and separtrix-to-wall gaps of ~5 cm at the outer midplane.

The first, #70224, is an unfueled pulse at high $I_p = 3.0$ MA ($B_\phi = 3.0$ T) with $P_{IN} \sim 20$ MW (supplied mostly by Neutral Beam Injection) and a plasma stored energy of $W_{plasma} \sim 8$ MJ. These discharges, discussed in detail in [7], have ITER-relevant pedestal collisionality, $\nu_e^* = 0.03$–0.08 ($n_{e,ped}$ and $T_{e,ped}$ at the pedestal top reach $\sim 6 \times 10^{19}\,\mathrm{m^{-3}}$ and ~2.5 keV, respectively) and extremely large, sporadic ELMs, with some events approaching an energy loss, $\Delta W_{ELM} \sim 1$ MJ. Such transients are thus close in amplitude to what is now thought to be necessary for the avoidance of material damage on ITER [8].

Upstream, the code is constrained by pedestal profile measurements from the new JET High resolution Thomson Scattering System (HRTS), the Lithium beam, ECE and CXRS diagnostics. At the targets, simulation results are compared with profiles of n_e and T_e obtained with the JET divertor Langmuir probe (LP) array.

The second, #58569, is a 2.0 MA, 2.4 T pulse with gas fuelling, $P_{IN} \sim 13$ MW and $W_{plasma} \sim 4$ MJ. In this case, $T_{e,ped} \sim 1.25$ keV and $n_{e,ped} \sim 4 \times 10^{19}\,\mathrm{m^{-3}}$ with $f_{ELM} \sim 30$ Hz and $\Delta W_{ELM} \sim 200$ kJ,

* Corresponding author.
E-mail address: barbora.gulejova@epfl.ch (B. Gulejová).
[1] See the Appendix of M.L. Watkins et al., Fusion Energy 2006 (Proc. 21st Int. Conf. Chengdu, 2006) IAEA, (2006).

0022-3115/$ - see front matter
doi:10.1016/j.jnucmat.2009.01.104

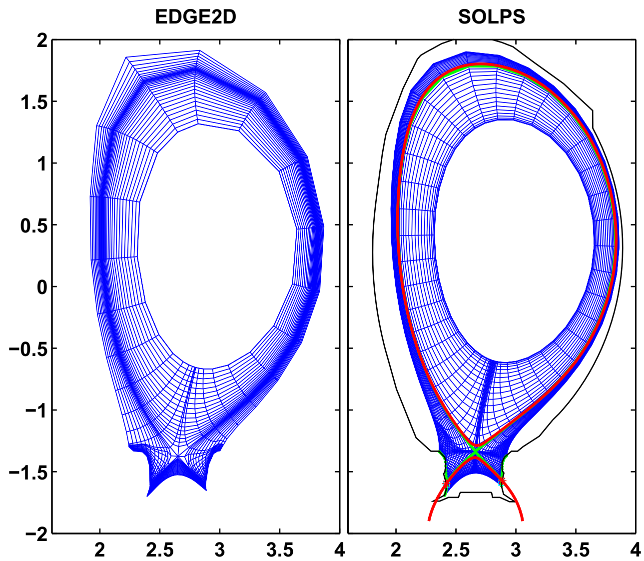

Fig. 1. Simulation grids, on the left: EDGE2D, on the right: SOLPS (red line = separatrix from EFIT, green line = SOLPS separatrix). (For interpretation of the references to colour in this figure legend, the reader is referred to the web version of this article.)

$\Delta W_{ELM}/W_{plasma} \sim 0.05$. As for the more recent pulse, the simulations are constrained upstream by experimental n_e, T_e and T_i profiles, but without the benefit (in terms of spatial resolution in the pedestal region) of the HRTS system, which had not yet been installed at the time of this earlier discharge. Unlike the higher power shot, however, this lower I_p discharge was run with a slow vertical sweep, allowing high resolution target profiles of ion flux density j_{sat}, n_e and T_e to be generated with the LP array (much higher than possible at higher I_p, where the risk of disruption is too high to allow large vertical movements). This particular discharge has been extensively modeled previously by Kallenbach et al. [1] with the EDGE2D-NIMBUS JET code package [9]. Reproducing this experiment-simulation comparison with SOLPS5 is an important aim of the work described here and is discussed in the following section.

3. Simulation of ELMing H-mode pulse #58569

3.1. Benchmark SOLPS vs. EDGE2D/NIMBUS

Although a benchmark of the SOLPS5 and EDGE2D-NIMBUS codes has previously been successfully attempted [10], the exercise reported here represents a more complex situation, in which impurities are included (all charge states of carbon) and a

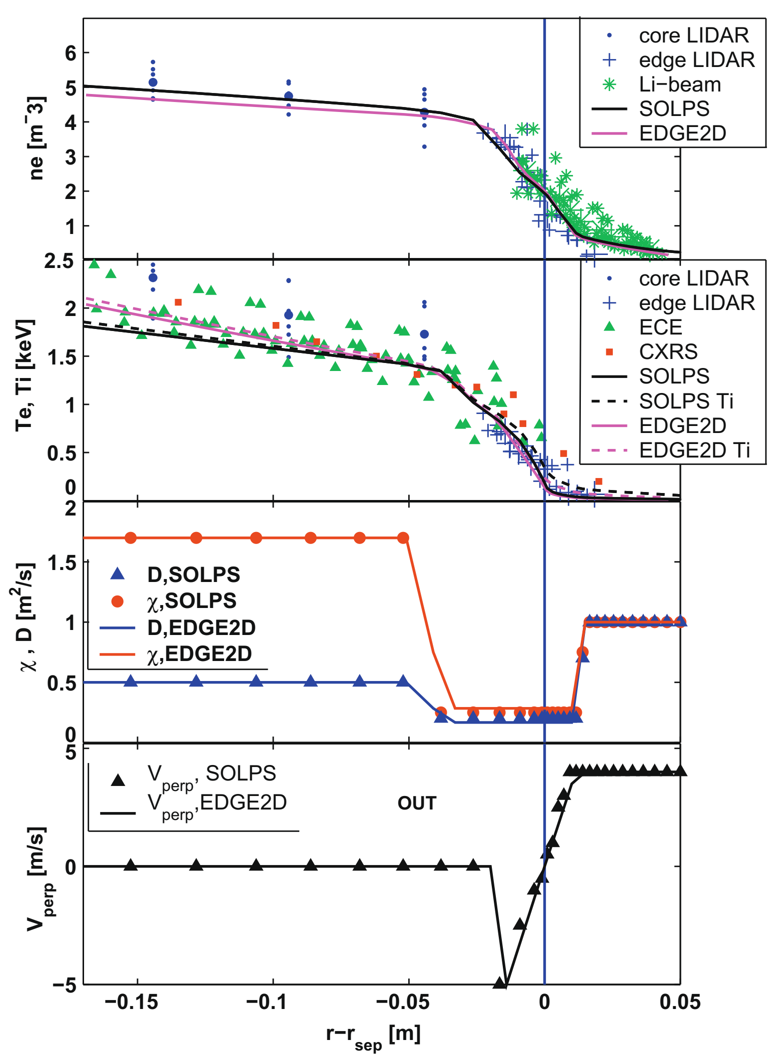

Fig. 2. Pre-ELM n_e, T_e, T_i upstream profiles for #58569, exp. data, SOLPS and EDGE2D, corresponding radial profiles of $D_\perp$, $\chi_{\perp e}$, $\chi_{\perp i}$, v_{perp}, where $\chi_{\perp e} = \chi_{\perp i} = \chi$.

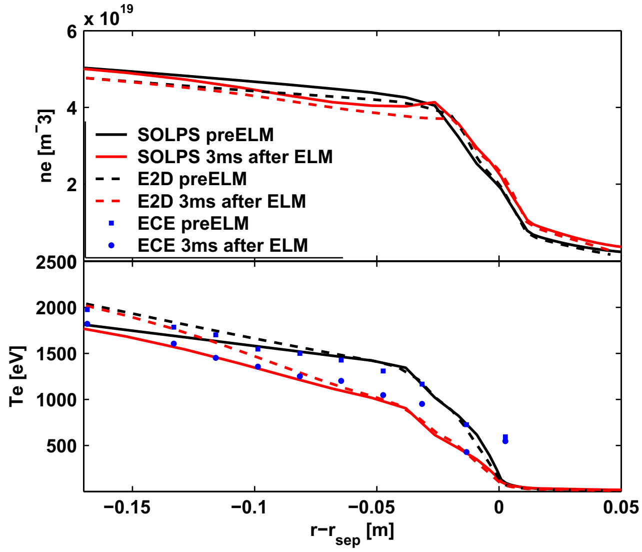

Fig. 3. Pre- ELM and ELM upstream profiles for #58569, up: n_e from SOLPS and EDGE2D, down: T_e from SOLPS, EDGE2D and ECE.

time-dependent solution is sought to capture the ELM. B2.5 and EDGE2D are stand-alone fluid codes solving the Braginskii equations for parallel transport with diffusive ansatz for cross-field transport. Each is interfaced with a neutral codes (EIRENE and NIMBUS) which may also be run independently but which differ considerably from each other. For example, NIMBUS uses a cylindrical and EIRENE a toroidal approximation and EIRENE includes a great deal more complexity in the various atomic physics processes that are accounted for. Each code package contains similar descriptions of physical and chemical sputtering. Even though the two code packages solve the overall edge fluid-neutral system in essentially the same way (i.e. based on a similar physics model), the codes are extremely complex and have been developed by many people over several years. Benchmarking one against the other is an important check of the overall level of consistency of two codes which solve the same problem with different numerical schemes. Since only one (SOLPS) has been used to provide a physics basis for the ITER divertor and SOL plasma [11], it is also important that the results of this code be checked against an independent package. The complexity of the time-dependent ELM case is such that a benchmark is even more important. One important difference is that time dependence is introduced in both the B2.5 and EIRENE components of SOLPS5 whilst in the EDGE2D/NIMBUS package only the fluid component is time dependent (neutrals are time independent). In EDGE2D the time-step increases during the ELM cycle from 10^{-4} s to 10^{-7} s, in B2.5 and EIRENE the same time step is applied throughout the simulation (in the case published here it was 10^{-5} s).

The highest level of complexity (namely the inclusion of drifts) is not attempted here since they were not included in the original EDGE2D-NIMBUS simulations [1].

Fig. 1 shows the two computational grids on which the ELMing H-mode benchmark has been performed. Both are derived from the magnetic flux surfaces obtained with the magnetic equilibrium reconstruction at 59 s using JET equilibrium code EFIT. The grids are not quite the same: the EDGE2D-NIMBUS grid has 48 cells poloidally, 30 radially and extends about 20 cm inside the separatrix (and 5 cm outside); the SOLPS5 grid has higher spatial resolution (96 cells poloidally and 36 cells radially) and extends much further into the core, ~40 cm. As far as possible, the benchmark is performed by setting all equivalent inputs in SOLPS5 as they were for the EDGE2D model in [1]. This includes wall albedos (recycling coefficients), parallel heat flux limits, separatrix density feedback (method to maintain the fixed value of the separatrix density at the midplane) and power fluxes in the ion and electron channels.

To model the pre-ELM steady state, a step-like ansatz is used for the radial profile of transport parameters exactly as performed in [1], within the small differences introduced as a consequence of the imperfect grid match. In this way, the inner core region, the

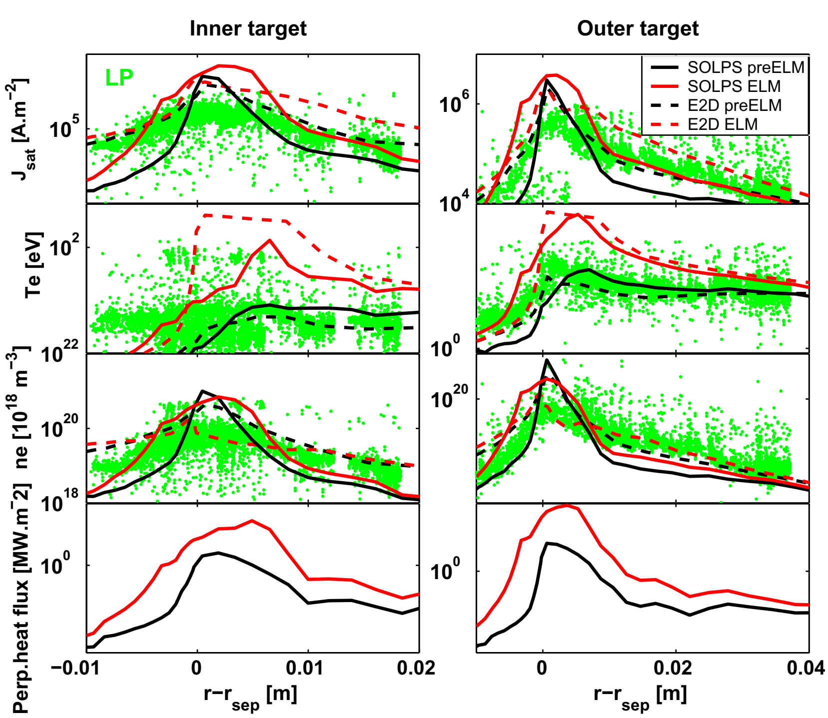

Fig. 4. Pre-ELM (black) and ELM (red) target profiles, j_{sat}, T_e, n_e from EDGE2D (dotted line) and SOLPS (solid line), experimental LP data (green), perp. heat fluxes only from SOLPS. (For interpretation of the references to colour in this figure legend, the reader is referred to the web version of this article.)

H-mode pedestal (edge transport barrier) and the outer SOL are represented as 3 distinct regions. However, in the divertor legs the profiles of the transport coefficients are flat (1 $m^2 s^{-1}$ for $D_\perp$, $\chi_{\perp e}$ and $\chi_{\perp i}$ and 0 m s^{-1} for v_{perp}).

For this ELM-free phase, the upstream profiles of n_e, T_e, T_i and transport coefficients ($D_\perp$, $\chi_\perp$ and v_{perp}) compiled in Fig. 2 (analogous to Fig. 2 in [1]) include the previous results obtained from [1], those from the new SOLPS5 simulation, and the experimental data (the experimental points have been processed slightly differently from those in [1] and may not correspond precisely). The high level of agreement between profiles from the two codes is extremely encouraging. Note that the heat conductivities $\chi_{\perp i}$ and $\chi_{\perp e}$ are assumed to be equal since there in no clear separation seen in T_i and T_e profiles. As described in [1], if diffusive outward transport is assumed, as it is here, an inward particle pinch is required (see Fig. 2) to match the experimental density profile. Not surprisingly, the same applies to the SOLPS5 simulations.

An approximation to the ELM cycle is included using an adhoc increase in transport coefficients for an ELM duration specified from experiment ~1 ms. Multiple ELMs are simulated as a repetitive increase of transport coefficients with frequency ~30 Hz. To match the observed $\Delta W_{ELM} \sim 200$ kJ, $D_\perp$, $\chi_{\perp e}$ and $\chi_{\perp i}$ are increased by factors of 20 and 40, respectively. This multiplication of the coefficients is applied everywhere poloidally, but radially only in the region extending from 5 cm inside the separatrix to 0.5 cm outside (and thus only in the very near SOL). Fig. 3 (analogous to Figs. 4(b) and 5 in [1]) compares the simulated upstream profiles of n_e and T_e from both codes, along with ECE data for T_e during the pre-ELM phase and 3 ms after the start of the ELM. The agreement between the two codes is again very reasonable, particularly in the pedestal region. The small difference in the core is most probably due to the deeper SOLPS simulation mesh.

At the divertor targets the code results are compared in Fig. 4 with the LP profiles obtained during the vertical strike point sweeps (analogous to Fig. 6 in [1] but now also including the inner target which was not given in [1]). Both inter-ELM and ELM profiles are plotted, where the latter corresponds to a point 40 µs after the transport coefficients are increased in the code. In the case of the LP data, all time points (ELM and inter-ELM) are included such that the lower and upper envelopes represent roughly the inter-ELM and ELM peak profiles. Agreement between the two codes, especially at the outer target, is again reasonable given, for example, the different neutral models. Both are a fair match to the experimental data but both largely over-estimate the target T_e, especially during the ELM and at the outer target. The T_e during the ELM at inner target predicted by SOLPS5 is much lower than the one from EDGE2D-NIMBUS and thus closer to the experimental data. Neither of he codes predicts much of a rise in peak density at the ELM, except the SOLPS at inner target. This is symptomatic of a problem in the ELM model itself and suggests that the conductive ansatz upstream should be replaced by a more convective transient. The differences described above might come from the mentioned different time-dependent treatment of the neutrals in the both codes. Fig. 4 also includes the SOLPS5 simulated inter-ELM and ELM target heat fluxes, computed assuming a total sheath transmission coefficient of $\gamma = 7.5$. Peak values during the ELM reach 100 and 300 MW m^{-2} at the inner and outer targets, respectively. The heat flux limits used are 5 for both electrons and for ions, so effectively no flux limits.

3.2. SOLPS analysis of ELM cycle energy balance

The SOLPS5 benchmark output has been used to study the energy balance during the ELM cycle (see Fig. 5). The measured time variation of the diamagnetic stored energy during the ELM cycles is well reproduced by the code, giving the observed $\Delta W_{ELM} \sim 200$ kJ. This energy is balanced by the calculated energy deposited on the targets ($E_{DEP} \sim 160$ kJ) and radiated energy ($E_{RAD} \sim 40$ kJ). A recent upgrade to the JET bolometer system has enabled radiated power measurements on ~1 ms timescale, allowing ELM induced radiation to be studied [7,12]. The ELM provokes an asymmetric radiation distribution favouring the inner divertor. An approximately linear dependence of this in-out asymmetry on ΔW_{ELM} is reported in [13] for discharges similar to this benchmark case, giving $E_{RAD,IN}/E_{RAD,OUT} \sim 2$ for $\Delta W_{ELM} \sim 200$ kJ. The SOLPS5 simulations match this ratio with $E_{RAD,IN}/E_{RAD,OUT} \sim 21$ kJ/10 kJ. The total radiation thus represents only ~20% of ΔW_{ELM}, the rest appearing as heat flux at the targets (in the code). In experiment, $\Delta E_{RAD}/\Delta W_{ELM} \sim 0.5$ [7,12,13]. The discrepancy is almost certainly due to the incomplete physics model of the ELM; experimentally it is known that the target energy deposition favours the inner target over the outer in the ratio 2:1 [13], whilst the code predicts $E_{IN}/E_{OUT} \sim 0.23$. It is also the case that co-deposited layers on the inner target enhance the impurity release due to the ELM (and hence the radiation) [7,12]. Such effects are not yet included in the codes.

4. SOLPS simulation of ELMing H-mode #70224

Following the same procedure as for the benchmark, preliminary attempts have been made to establish an ELM-free baseline

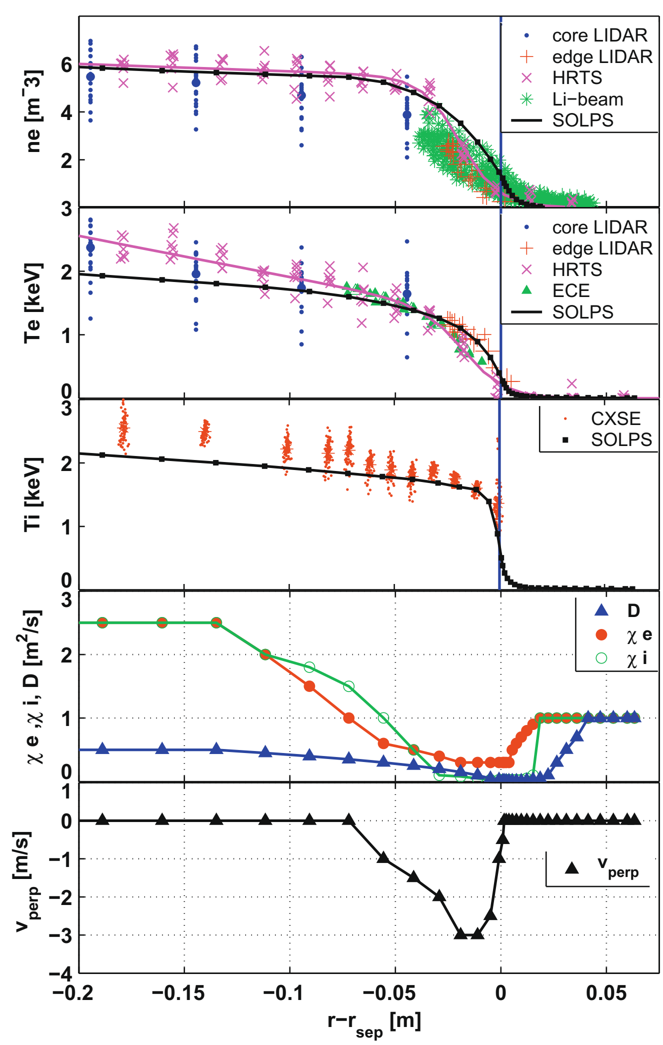

Fig. 5. Pre-ELM upstream n_e, T_e, T_i profiles for #70224, exp. data and SOLPS, corresponding radial profiles of $D_\perp$, $\chi_{\perp e}$, $\chi_{\perp i}$, v_{perp}.

simulation for a 3.0 MA, high stored energy discharge (#70224) in which a few extremely large ELMs occur (ΔW_{ELM} approaching 1 MJ). As before, poloidal drifts are switched off and a very deep grid, extending 40 cm into the core, is used. These higher I_p shots have low pedestal collisionality and operate at low density ($n/n_{GW} \sim 0.4$). In this case, as seen in Fig. 5, where the upstream experimental and simulated profiles are presented, $T_i \neq T_e$ in the pedestal region, nor do they have the same profile shape. This is contrast to the benchmark case at higher fuelling and lower density, where $T_i \sim T_e$ throughout the profile.

To achieve a reasonable match between code and experiment, values of $D_\perp = 0.01$, $(1)\,m^2\,s^{-1}$, $\chi_{\perp e} = 0.3$, $(1)\,m^2 s^{-1}$ are required in the pedestal, (SOL) regions, respectively. To match the very steep T_i pedestal, $\chi_{\perp i} = 0.03$, $(1)\,m^2\,s^{-1}$ in the pedestal, (SOL) region are required. Variation of the ratio $\chi_{\perp e}/\chi_{\perp i}$ (assuming ion-electron energy equipartition) was sufficient to find a reasonable fit to the experimental profiles. In common with the lower power benchmark pulse, an inward particle pinch appears to be required in the pedestal region if the experimental density profile is to be matched. It also appears to be a feature of high power H-mode shots on JET since similar modeling with SOLPS5 of ELMing H-mode discharges on ASDEX Upgrade [14] and TCV [15] did not require a finite $v_\perp$.

At the targets, agreement between code and experiment is fair (not shown), although the lack of vertical strike point sweeps means that there are only a few points on the radial (LP) profiles of T_e and n_e. At these high power levels, there is unfortunately no data in the main SOL with which to better constrain the transport coefficients there. This inter-ELM solution is a good basis for planned time-dependent ELM simulations.

5. Conclusions

Two high power JET H-modes with $\Delta W_{ELM} \sim 200$ kJ and $\sim$1 MJ have been simulated with SOLPS5, using upstream experimental pedestal profiles to constrain the code. One of the cases has been exhaustively modeled in earlier work with the EDGE2D-NIMBUS code [1], so that these new SOLPS5 simulations may be used to benchmark the two codes. Good agreement has been found in the results examined thus far – an encouraging outcome given the relative complexity of the benchmark, which includes carbon impurities and a time dependent, multiple ELM cycle simulation. Analysis of the energy balance during the ELM with SOLPS5 shows $\sim$20% of ΔW_{ELM} is radiated, with a 2:1 asymmetry favouring the inner divertor. Although this radiation asymmetry is also seen experimentally, the predicted fractional radiated energy is rather lower than observed and the ratio of energy deposited on the targets found in the code favours the outer target, in contradiction to that found experimentally, demonstrating that the simple model of the ELM used here is incomplete. For a second pulse, with twice the stored energy as the benchmark case, only the inter-ELM phase has been simulated. In both cases, a strong inward particle pinch in the pedestal region is found to be necessary to match the steep upstream density pedestal.

Acknowledgements

This work was conducted under the European Fusion Development Agreement and was supported in part by the Swiss National Science Foundation, EURATOM and the UK Engineering and Physical Sciences Research Council.

References

[1] A. Kallenbach et al., Plasma Phys. Control. Fus. 46 (2004) 431.
[2] R. Schneider et al., Contribution Plasma Phys. 46 (1) (2006) 3.
[3] A. Kukushkin et al., Nucl. Fus. 43 (2003) 716.
[4] B.Gulejova et al., in: Proceedings of EPS 2007, Warsaw, Poland, paper P1.044.
[5] D. Coster, J. Nucl. Mater. 390–391 (2009) 826.
[6] A. Loarte et al., Phys. Plasmas 11 (2004) 2668.
[7] R. Pitts et al., J. Nucl. Mater. 390–391 (2009) 755.
[8] J. Roth, J. Nucl. Mater. 390–391 (2009) 1.
[9] R. Simonini et al., Contribution Plasma Phys. 34 (1994) 368.
[10] D. Coster et al., J. Nucl. Mater. 337–339 (2005).
[11] A. Kukushkin et al., Nucl. Fus. 45 (2005) 608.
[12] A. Huber et al., J. Nucl. Mater. 390–391 (2009) 830.
[13] R. Pitts et al., Nucl. Fus. 47 (2007) 1437.
[14] A. Chankin et al., Plasma Phys. Control. Fus. 48 (2006) 839.
[15] B. Gulejova et al., J. Nucl. Mater. 363–365 (2007) 1037.